PCCP

COMMUNICATION

View Article Online
View Journal | View Issue

Cite this: *Phys. Chem. Chem. Phys.*, 2016, **18**, 15510

Received 18th April 2016,
Accepted 13th May 2016

DOI: 10.1039/c6cp02596j

www.rsc.org/pccp

Tip enhanced Raman spectroscopy imaging of opaque samples in organic liquid†

T. Touzalin, A. L. Dauphin, S. Joiret, I. T. Lucas* and E. Maisonhaute*

Implementation of Tip Enhanced Raman Spectroscopy in liquid is still a challenge. We demonstrate herein its feasibility in an upright illumination/collection configuration. Through a thin layer of organic solvent covering the sample, laser focussing on the tip is possible, enabling TERS imaging in liquid.

Introduction

Beyond topography resolved at a sub-molecular scale, methodologies derived from Scanning Probe Microscopy (SPM) provide a range of useful information about the electrical, optical, mechanical or magnetic properties of the sample under scrutiny.[1] SPM can be implemented under various environments ranging from low temperature and ultra-high vacuum conditions to liquid media. This versatility accounts for the very broad scientific area covered by SPM. In research domains like molecular electronics or biology, the stringent need for additional chemical identification at the molecular scale has been so far addressed by UHV Inelastic Scanning Tunneling Spectroscopy derived from Scanning Tunneling Microscopy (STM) or methods derived from Atomic Force Microscopy, for example force spectroscopy.[2]

Near-field scanning optical microscopy (NSOM) associating vibrational spectroscopy (Raman, infrared: IR) and SPM stands as a powerful alternative by providing unambiguous and more precise chemical identification with high sensibility and high spatial resolution. IR-NSOM has been a fast emerging technology, due to the strong IR signature of most compounds and the availability of suitable probes, but its implementation in liquids is really tedious due to the strong IR absorption of usual solvents.[3–6] In parallel, the development of Raman-SNOM, *i.e.* Tip Enhanced Raman Spectroscopy (TERS),[7,8] has necessitated tailoring specific probes which support localized surface plasmon resonance close to the apex of the tip, at the so-called "hot spot".[9] When a visible laser light of suitable wavelength is shined on a gold or silver tip, the electric field at the hot spot is considerably amplified and translates into a strong near field Raman scattering signal enhancement at the tip/sample interface.[10–14] Low laser excitation power can be therefore applied, minimizing considerably the far-field contribution to the scattered signal. The strong signal enhancement compensates for the low efficiency of the inelastic scattering process of many compounds, enabling detection and imaging of single molecules.[15,16] While silver provides the largest enhancement, gold is less prone to oxidation and therefore more adapted to liquids.[11,17,18]

However, implementation of TERS in liquid also brings out other difficulties. The main one is the delicate optical alignment to achieve accurate focusing of the laser beam on the tip apex and also to ensure an efficient collection of the scattered signal especially through a layer of liquid. Most literature reports describe transparent samples set on an inverted optical microscope; focusing of the laser beam on the TERS probe is therefore easily achieved directly through the sample.[19–23] With opaque samples that necessitate top or side illumination/collection, the optical signal is inevitably deviated and considerably attenuated by refraction at each interface. Ren *et al.* recently elegantly circumvented this problem by mounting the sample in a liquid cell equipped with a side thin glass window and obtained an efficient side illumination of a STM probe enabling single point TERS spectroscopy of a pyridinyl derivative in water.[24] The window was positioned about 1 mm apart from the probe. This solution unfortunately freezes the tip *vs.* sample/window positioning, obliterating TERS sample imaging capabilities in liquid. Moreover for further development of TERS in organic solvent, even single point spectroscopy through 1 mm of liquid is not conceivable. We therefore propose in this work an upright illumination/collection configuration that enables TERS imaging in organic liquid (hexadecane).

Sorbonne Universités, UPMC Univ Paris 06, UMR 8235, Laboratoire Interfaces et Systèmes Electrochimiques, F-75005 Paris, France. E-mail: ivan.lucas@upmc.fr, emmanuel.maisonhaute@upmc.fr

† Electronic supplementary information (ESI) available: Materials and methods, supplementary Raman spectra and *XY* objective scan maps. See DOI: 10.1039/c6cp02596j

Results and discussion

In our setup described in Fig. 1, a polarized excitation laser (λ_{exc} = 632.8 nm) is focused on the STM probe apex through a long distance 100× objective (working distance: 6 mm) with high numerical aperture (N.A. = 0.7). Therefore, the STM tip holder can fit between the objective and the sample. An electronic micrograph of a typical tip is presented in Fig. 1b. A gold tip is bent with an angle of 30 to 45° to the normal of the sample as previously depicted by Zenobi *et al.* in air.[25,26] This angle allows the apex of the tip to reach the focal point of the objective for an optimized signal collection and enables a better alignment of the electric field along the shaft of the tip. This also maintains the imaging capability of the STM probe. The objective is mounted onto a piezo positioning system which allows an accurate screening of the optical hotspot on the gold tip, *i.e.* the position of the laser on the tip giving the maximum enhancement of the Raman signal intensity.

The TERS signal of the thioazobenzene derivative **1** (see Fig. 2) self-assembled on a gold surface was first collected in air. The sample was prepared by soaking a gold substrate in a 0.2 mM ethanolic solution of **1**, followed by immersion in pure ethanol for 1 h in order to remove any physisorbed molecule (see ESI† for more details). Screening of the tip hotspot is achieved by performing an objective mapping, *i.e.* a raster scanning of the objective in the directions parallel (*XY*) and normal (*XZ*, *YZ*) to the sample surface synchronized with the registering of the overall Raman signal intensity, while maintaining the tip at the tunnel contact with the sample. Fig. 2a displays two Raman spectra of **1** collected at the exact hot spot location and also slightly away, highlighting respectively the strong near field signal (TERS) and the extremely weak far-field contribution (microRaman) using only 14.1 μW of laser power. Particularly, the bands at 1143, 1415, 1443 and 1465 cm^{-1} appear with a large signal/noise ratio as already reported in the literature.[27,28] The far field signal collected with a higher laser power and longer exposure time is presented in Fig. S1 of ESI.† A typical Raman mapping of the integrated spectrum intensity between 1394 and 1495 cm^{-1} during a *XY* objective map is presented in Fig. 2b and confirms the strong enhancement of the signal around the hotspot location and the abrupt drop of the intensity in its close proximity (600 nm).

Then, a thin layer of liquid hexadecane was added onto the sample. This sample/solvent combination represents an ideal system to evaluate the possible screening of the sample signal by the surrounding solvent since the Raman spectrum of pure hexadecane presented in Fig. S2 of ESI,† displays several bands that overlap with those of **1**. Using this specific solvent that has a low dielectric constant, no electrical insulation of the STM tip is required to avoid current leakage due to electrochemical reactions during tip polarization. The main limitation of our configuration lies in the tip/liquid meniscus that interferes with the optical path. The height and radius of curvature of this meniscus strongly depends on the diameter and angle of the tip. We observed that a liquid thickness of a few micrometers (2–20 μm) however still allowed an accurate focusing of the laser on the tip. Under such conditions, search of the hot spot in liquid became possible as revealed by the *XY* objective map depicted in Fig. 3a. The spectra at the exact hotspot (blue) and slightly off (red) appear in Fig. 3b. A weak contribution from the solvent is apparent on all collected spectra as revealed on the average spectrum collected for a large area of the Raman map outside the hot spot (black spectra). At the hot spot however, the contribution from **1** largely dominated, demonstrating for the first time that TERS is effective in hexadecane.

To show that our setup is also suitable for TERS imaging in liquid, a 300 × 300 nm^2 area of the sample was scanned in

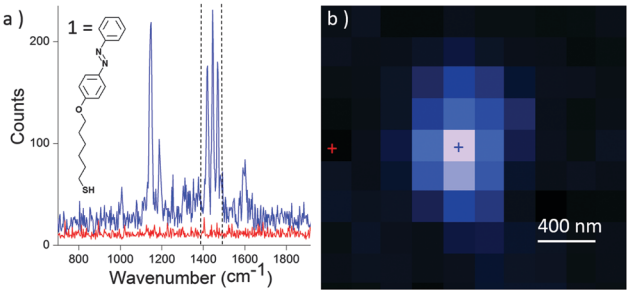

Fig. 2 STM-TERS experiment performed in air: (a) raw Raman spectra collected at the exact hot spot location (blue: "TERS") and slightly away (red: "μRaman"). Laser power: 14.1 μW; acquisition time: 100 ms; STM setpoint current: 200 pA; 0.1 V bias. (b) 2 × 2 μm^2 *XY* objective map obtained by integration of the peak intensity (with baseline correction) between 1394 and 1495 cm^{-1} revealing the location of the hot spot on the tip.

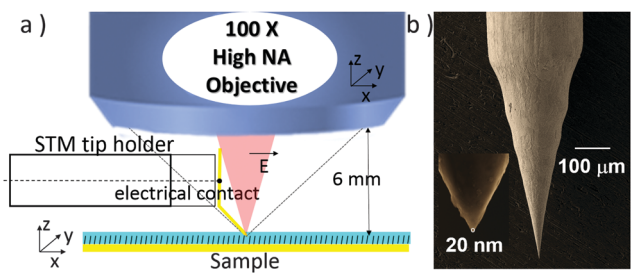

Fig. 1 (a) Upright illumination/collection set-up that enables STM-TERS imaging in a thin layer of organic liquid (hexadecane), (b) electrochemically etched gold wire used as a STM tip (radius of curvature < 20 nm).

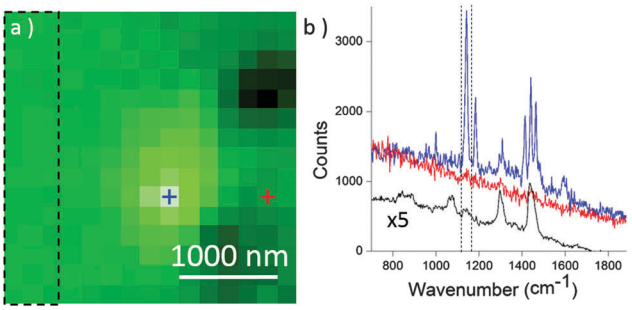

Fig. 3 STM-TERS experiment performed in a thin layer of liquid hexadecane: (a) 3 × 3 μm^2 *XY* objective map (integration of the peak intensity with baseline correction between 1125 and 1162 cm^{-1}), (b) Raman spectra at the exact hot spot location on the tip (blue: TERS) and slightly apart (red: μRaman), and averaged spectrum for the dashed rectangle area of the objective map. Laser power: 287 μW; acquisition time: 500 ms; STM setpoint current: 1000 pA (0.1 V bias).

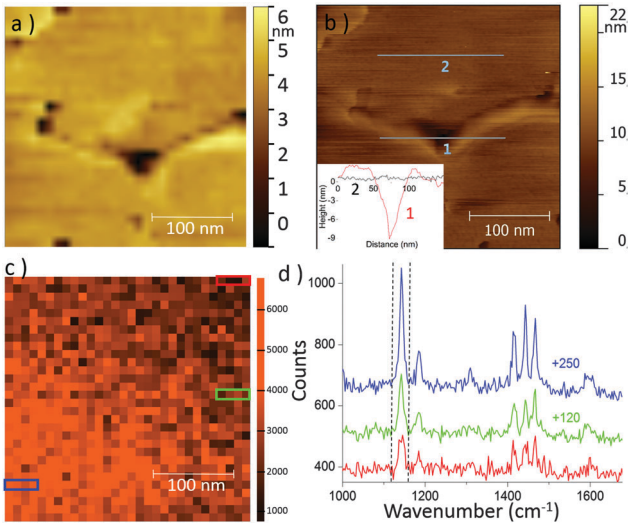

Fig. 4 TERS imaging performed in liquid hexadecane. (a) Low resolution STM image (30 × 30 pixels^2) obtained simultaneously with TERS mapping, STM set point current: 500 pA and bias: 0.1 V. (b) High resolution (256 × 256 pixels^2) STM image obtained after TERS mapping. Inset: 2 topographic profiles. (c) 30 × 30 pixels^2 TERS map in liquid – integration of the band between 1125 and 1162 cm^{-1} after baseline correction. Laser power: 98 μW; acquisition time: 107 ms. (d) Raw TERS spectra averaged (without baseline subtraction) the blue, green and red rectangles areas on (c). Spectra are offset for clarity.

STM mode in hexadecane while recording TERS spectra. With a 30 × 30 pixels^2 image and 0.107 s acquisition time per spectrum (laser power = 98 μW), recording a full TERS image took only 97 s. A higher resolution STM image (256 × 256 pixels) was also recorded immediately after. In Fig. 4, the comparison between low and high resolution STM images shows that a 30 × 30 pixels^2 image is sufficient to evidence topography details, like pin holes present over the gold surface. Furthermore, in the high resolution image, the topography is well-described meaning that the STM-TERS tip was sharp enough to minimize convolution effects.

A TERS map obtained by integrating the band intensity of **1** between 1125 and 1162 cm^{-1} is presented in Fig. 4c. It reveals that the signal intensity on the lower left part of the image is more intense. Such local intensity fluctuations would never be detected in microRaman. Fig. 4d displays three spectra obtained by averaging the 4 consecutive spectra inside the 3 three different colored rectangles indicated in Fig. 4c. The lower intensity corresponds to 40% of the highest one. Note that the scan proceeded from left to right and bottom to top. To explain the drop in intensity along the vertical direction of the raster scan, a change in the laser focusing on the tip may be invoked. This could originate from thermal effect induced by laser irradiation, altering either the refraction at the air/liquid interface or the meniscus height. Two *XY* objective maps recorded before and after TERS mapping of the sample (Fig. S3, ESI†), within a 17 min interval, show however a signal loss of at most 20% but also a slight shift of the hot spot position (at most 200 nm). This slight progressive defocusing cannot therefore account for all the signal fluctuation on the TERS sample map. Furthermore, defocusing of the laser cannot be responsible for variations along the horizontal direction. We therefore rather incriminate a local variation in the surface coverage of **1** due to non-homogenous SAM formation on gold, possibly combined with a modification of the molecular orientation of **1** on the surface. This is probably due to the SAM preparation.[27,28] As a consequence of this surface concentration change, no relation between the topography and the Raman intensity could be clearly established.[29,30] This experiment illustrates that TERS imaging is operational in organic solvent using an upright configuration. The next stage will be to precisely determine the spatial resolution of TERS in liquid by imaging small nanoobjects in a similar way to what was recently performed in air with carbon nanotubes.[31]

Conclusions

This work demonstrates that it is possible, using an upright optical configuration, to implement TERS imaging of an opaque sample in contact with an organic liquid, with fast acquisition time and minimal laser power. With this set-up, the efficient excitation/collection of the scattered Raman signal enables extraction of the chemical signature of a molecular monolayer from the one of the surrounding solvent. To achieve such performances, the liquid thickness has to be optimized (around 20 μm at most here), in order to reduce the distortion of the optical path and the loss of signal at the tip/liquid interface (meniscus). These promising results pave the road to TERS imaging in other solvents or electrolytes.[22,24,32–34]

Acknowledgements

This work was funded by UPMC, CNRS, the FP7-People program (CIC) of the European union, the Labex "MiChem" (ANR-11-IDEX-0004-02) and the Region Ile de France through the framework DIM Nano-K. We also thank Dr. Marc Chaigneau (Horiba) for helpful discussion.

References

1 C. J. Chen, *Introduction to Scanning Tunneling Microscopy*, Oxford University Press, Oxford, 2nd edn, 2007.
2 J. Landoulsi and V. Dupres, *Phys. Chem. Chem. Phys.*, 2013, **15**, 8429–8440.
3 A. Deniset-Besseau, C. B. Prater, M. J. Virolle and A. Dazzi, *J. Phys. Chem. Lett.*, 2014, **5**, 654–658.
4 S. Heedy, M. Lo, E. Dillon, Q. C. Hu, C. Prater, R. Shetty, K. Kjoller, C. Marcott, A. Dazzi and C. Yip, *Biophys. J.*, 2014, **106**, 205A.
5 I. T. Lucas, A. S. McLeod, J. S. Syzdek, D. S. Middlemiss, C. P. Grey, D. N. Basov and R. Kostecki, *Nano Lett.*, 2015, **15**, 1–7.
6 O. Khatib, J. D. Wood, A. S. McLeod, M. D. Goldflam, M. Wagner, G. L. Damhorst, J. C. Koepke, G. P. Doidge, A. Rangarajan, R. Bashir, E. Pop, J. W. Lyding, M. H. Thiemens, F. Keilmann and D. N. Basov, *ACS Nano*, 2015, **9**, 7968–7975.

7 B. Pettinger, G. Picardi, R. Schuster and G. Ertl, *Electrochemistry*, 2000, **68**, 942–949.
8 R. M. Stockle, Y. D. Suh, V. Deckert and R. Zenobi, *Chem. Phys. Lett.*, 2000, **318**, 131–136.
9 X. Wang, Z. Liu, M. D. Zhuang, H. M. Zhang, Z. X. Xie, D. Y. Wu, B. Ren and Z. Q. Tian, *Appl. Phys. Lett.*, 2007, **91**, 101105.
10 Z. Yang, J. Aizpurua and H. Xu, *J. Raman Spectrosc.*, 2009, **40**, 1343–1348.
11 E. C. Le Ru and P. G. Etchegoin, *Principles of Surface Enhanced Raman Spectroscopy and related phenomena*, Elsevier Science Bv, Amsterdam, 2009.
12 T. Schmid, L. Opilik, C. Blum and R. Zenobi, *Angew. Chem., Int. Ed.*, 2013, **52**, 5940–5954.
13 L. Langeluddecke, P. Singh and V. Deckert, *Appl. Spectrosc.*, 2015, **69**, 1357–1371.
14 C. Blum, L. Opilik, J. M. Atkin, K. Braun, S. B. Kammer, V. Kravtsov, N. Kumar, S. Lemeshko, J. F. Li, K. Luszcz, T. Maleki, A. J. Meixner, S. Minne, M. B. Raschke, B. Ren, J. Rogalski, D. Roy, B. Stephanidis, X. Wang, D. Zhang, J. H. Zhong and R. Zenobi, *J. Raman Spectrosc.*, 2014, **45**, 22–31.
15 W. H. Zhang, B. S. Yeo, T. Schmid and R. Zenobi, *J. Phys. Chem. C*, 2007, **111**, 1733–1738.
16 R. Zhang, Y. Zhang, Z. C. Dong, S. Jiang, C. Zhang, L. G. Chen, L. Zhang, Y. Liao, J. Aizpurua, Y. Luo, J. L. Yang and J. G. Hou, *Nature*, 2013, **498**, 82–86.
17 P. Aubertin, M. Aissa, N. Raouafi, S. Joiret, A. Courty and E. Maisonhaute, *Nano Res.*, 2015, **8**, 1615–1626.
18 E. Sutter, K. Jungjohann, S. Bliznakov, A. Courty, E. Maisonhaute, S. Tenney and P. Sutter, *Nat. Commun.*, 2014, **5**, 4946.
19 C. Hoppener and L. Novotny, *Nano Lett.*, 2008, **8**, 642–646.
20 C. Hoppener and L. Novotny, *Nanotechnology*, 2008, **19**, 384012.
21 A. Nakata, T. Nomoto, T. Toyota and M. Fujinami, *Anal. Sci.*, 2013, **29**, 865–869.
22 D. Kurouski, M. Mattei and R. P. Van Duyne, *Nano Lett.*, 2015, **15**, 7956–7962.
23 T. Schmid, B. S. Yeo, G. Leong, J. Stadler and R. Zenobi, *J. Raman Spectrosc.*, 2009, **40**, 1392–1399.
24 Z.-C. Zeng, S.-C. Huang, D.-Y. Wu, L.-Y. Meng, M.-H. Li, T.-X. Huang, J.-H. Zhong, X. Wang, Z.-L. Yang and B. Ren, *J. Am. Chem. Soc.*, 2015, **137**, 11928–11931.
25 J. Stadler, T. Schmid and R. Zenobi, *Nano Lett.*, 2010, **10**, 4514–4520.
26 J. Stadler, B. Oswald, T. Schmid and R. Zenobi, *J. Raman Spectrosc.*, 2013, **44**, 227–233.
27 G. Picardi, M. Chaigneau, R. Ossikovski, C. Licitra and G. Delapierre, *J. Raman Spectrosc.*, 2009, **40**, 1407–1412.
28 H. K. Wickramasinghe, M. Chaigneau, R. Yasukuni, G. Picardi and R. Ossikovski, *ACS Nano*, 2014, **8**, 3421–3426.
29 P. Z. El-Khoury, Y. Gong, P. Abellan, B. W. Arey, A. G. Joly, D. H. Hu, J. E. Evans, N. D. Browning and W. P. Hess, *Nano Lett.*, 2015, **15**, 2385–2390.
30 W. H. Zhang, X. D. Cui, B. S. Yeo, T. Schmid, C. Hafner and R. Zenobi, *Nano Lett.*, 2007, **7**, 1401–1405.
31 C. Chen, N. Hayazawa and S. Kawata, *Nat. Commun.*, 2014, **5**, 3312.
32 V. Climent, J. D. Zhang, E. P. Friis, L. H. Ostergaard and J. Ulstrup, *J. Phys. Chem. C*, 2012, **116**, 1232–1243.
33 X. S. Zhou, B. W. Mao, C. Amatore, R. G. Compton, J. L. Marignier, M. Mostafavi, J. F. Nierengarten and E. Maisonhaute, *Chem. Commun.*, 2016, **52**, 251–263.
34 P. Fortgang, E. Maisonhaute, C. Amatore, B. Delavaux-Nicot, J. Iehl and J. F. Nierengarten, *Angew. Chem., Int. Ed.*, 2011, **50**, 2364–2367.